

# Probing the Structure of Dark Matter in Galaxy Halos and Clusters using Supernovae

R. Benton Metcalf

*Institute of Astronomy, University of Cambridge  
Madingley Road Cambridge CB3 0HA, UK*

## ABSTRACT

A new method for measuring gravitational lensing with high redshift type Ia supernovae is investigated. The method utilizes correlations between foreground galaxies and supernova brightnesses to substantially reduce possible systematic errors and increase the signal to noise ratio. It is shown that this lensing signal can be related to the mass, size and substructure of galaxy halos and galaxy clusters if dark matter consists of microscopic particles. This technique may be particularly useful for measuring the size of dark matter halos, a measurement to which the lensing of galaxies is not well suited, and for measuring the level of substructure in galaxy halos, a problematic prediction of the cold dark matter model. The contributions to the signal from galaxy halos and galaxy clusters are modeled and contributions to the noise from fluctuations in the galaxy number counts, galaxy redshift error, dispersion in SN luminosities and sample variance are estimated. The intrinsic distribution of supernova luminosities and its redshift evolution are removed as major sources of uncertainty. The method is found to be complimentary to galaxy–galaxy lensing. The required observations of  $\gtrsim 100$  supernovae have already been proposed for the purposes of cosmological parameter estimation.

*Subject headings:* Cosmology, Dark Matter, Gravitational Lensing, Supernovae

## 1. Introduction

Outside of the visible extent of galaxies not a great deal is known about the distribution of dark matter (DM) on scales smaller than galaxy clusters. Galaxy–galaxy lensing (Fischer et al. 1999; Hudson et al. 1998; Brainerd, Blandford, & Smail 1996; Griffiths et al. 1996; Tyson et al. 1984) and studies of the satellite galaxies orbiting the Milky Way and other galaxies (Wilkinson & Evans 1999; Kochanek 1996; Zaritsky & White 1994) have put some constraints on the mass of galaxy halos, but their size scale and the degree to which they are smooth mass distributions or collections of subclumps are not well determined. Even the concept of galaxy halos, with a single galaxy within each of them and well defined sizes, may not be correct. Nor is it clear how the observable properties of galaxies relate to the DM around them. It would be preferable if these properties could be derived directly from cosmological initial conditions and the properties of DM, but this has proven to be an extremely difficult problem. Simulations of galaxy formation give incomplete answers which are hard to compare with observations. For example pure cold dark matter (CDM) simulations contain a large amount of small scale structure which is not mirrored in the observed distribution of light (Moore et al. 1999a). The process of galaxy formation is highly dependent on cooling and feedback from stars which must be modeled ad hoc. As a result complete galaxies have never been created in a hydrodynamic simulation. In addition, changing the properties of DM so that it is self-interacting or a mixture of hot and cold DM, for example, can have a strong influences on small scale structure. The theory of galaxy formation, and DM, would clearly benefit from further observational constraints on these scales. Gravitational lensing is presently the most promising method available for probing the distribution of dark matter and its relationship with light.

The discovery of a tight correlation between the light curve shape and the luminosities of type Ia supernovae (SNe) has resulted in their great utility as cosmological distance indicators (Hamuy et al. 1996; Riess, Press, & Kirshner 1996) and as a possible probe of gravitational magnification. The measured standard deviation of corrected peak luminosities in local SNe is now  $\lesssim 0.12$  mag. Two groups have used these SNe to constrain the distance–redshift relation and through this cosmological parameters (Perlmutter et al. 1997; Riess et al. 1998). The successes of these studies have inspired plans for more aggressive, larger searches for high redshift SNe in the near future. The volume and quality of data is likely to increase dramatically. These data will have implications well beyond constraints on  $\Omega_m$  and  $\Omega_\Lambda$  – the average mass density and vacuum energy density. Other uses include measuring the universe’s equation of state and star formation history. Here I discuss the gravitational lensing of high redshift SNe and its implications for dark matter, its distribution and its correlation with light.

Metcalf & Silk (1999) have already discussed using the lensing of SNe to determining the composition of DM. It was found that DM made predominantly of macroscopic compact objects with masses  $\gtrsim 10^{-3} M_\odot$  (ex. MACHOs, primordial black holes) can be differentiated from DM made of microscopic particles (ex. WIMPs, axions) through studying the magnification probability distribution of  $\sim 100$  SNe at  $z \sim 1$ . In the case of macroscopic DM, the most likely brightness of a supernova (SN) is well below the mean value, and near the empty beam solution or Dyer–Roeder distance (Dyer & Roeder 1974). Seljak & Holz (1999) expanded on this work by considering a mixture of macroscopic and microscopic DM. Unknown to the author, Rauch (1991) had previously suggest this use for type Ia SNe, but had not investigated the shift in the mode of the distribution to values below the standard Friedmann–Robertson–Walker luminosity distance. Instead he concentrated on the detection of rare high magnification events and concluded that many more SNe would be require to detect macroscopic compact objects. In this paper only microscopic DM is considered. In this case the DM can be treated as a transparent, massive fluid clumped into structures that are much larger than the angular size of the source.

A few authors have considered how the lensing of type Ia SNe could be used to probe DM structure. Kolatt & Bartelmann (1998) pointed out that the mass sheet degeneracy of galaxy cluster shear maps could be broken with SNe. Porciani & Madau (2000) calculated the probability of strong lensing events in a CDM universe. They used the Press–Schechter prediction for the mass function of halos and find the optical depth for a certain magnification threshold. High magnification events are rare ( $\sim 2 \times 10^{-3}$  chance for magnification above 1.3 at  $z_s = 1$ ) although they could be specifically searched for by monitoring high–mass galaxy clusters. The approach discussed in this paper incorporates both strongly and weakly lensed SNe to take better advantage of the data and broaden the sensitivity to mass outside halo cores hence probing the size scale of the extended DM distribution. The author has previously pointed out that lensing by microscopic DM could be detected by an increase in the variance of SN brightnesses at high redshift (Metcalf 1999). In addition this increase in dispersion is important for determining the noise in cosmological parameter estimates when using SNe at  $z \sim 1$ . The feasibility of measuring lensing via this method is potentially hampered by uncertainties in the intrinsic distribution of SN luminosities and its possible redshift dependence. In this paper, I seek to eliminate these systematic errors by correlating SN brightnesses with foreground galaxies. In this way a null result is expected in the absence of lensing. This approach also makes interpretation of the result more straightforward and results in significantly higher signal to noise. This work is an extension and improvement an earlier parametric approach summarized in Metcalf (1998).

In section 2 the first order correlation statistic is defined. In section 3 models are constructed for estimating and interpreting the contribution of galaxy halos (3.1) and extragalactic clustering (3.2) to the lensing signal. Sources of noise are considered in section 4. Some higher order correlation statistics are discussed in section 5. The lensing of SNe is compared to the lensing of galaxies in section 6. The final section contains a summary and discussion of future prospects.

## 2. Correlating SNe with Foreground Light

As stated above I seek to reduce as much as possible the influence of SN redshift evolution by considering only correlations in foreground light and SN brightness. Using statistics based on these correlations also increases the signal to noise and allows for simple interpretations of the results in terms of mass–light correlations. Throughout this paper units are used in which the speed of light,  $c = 1$ .

To start, consider the weighted flux from foreground galaxies

$$\mathcal{F} = \sum_i w(z_i, z_s, y_i) f_i \quad (1)$$

where  $y_i$  is the proper distance separating the galaxy  $i$  from the line-of-sight to the SN,  $f_i$  is the flux received from that galaxy and  $z_s$  is the redshift of the source SN. An attempt should be made to correct the  $f_i$ 's for extinction and inclination effects as well as k-corrections so that  $f_i$  accurately reflects the intrinsic luminosity of the galaxy. I will choose the weight function to be factorable and normalized as follows

$$w(z, z_s, y) = w_1(z, z_s) w_2(y) \quad (2)$$

$$\int_0^{z_s} dz w_1(z, z_s) = 1 \quad , \quad 2\pi \int_0^\infty dy y w_2(y) = 1.$$

This gives  $\mathcal{F}$  the units of flux per area. Besides these constraints the weighting function is arbitrary so that it can be adjusted to maximize the signal to noise. Later I will make a particular choice of weighting function for numerical calculations.

For simplicity I will consider a flux limited sample of foreground galaxies. In this case the average of  $\mathcal{F}$  is

$$\overline{\mathcal{F}} = \int_0^{z_s} dz w_1(z, z_s) \frac{\overline{f}(z) \eta(z)}{(1+z)} \frac{d\chi}{dz}(z) = \frac{1}{4\pi H_o} \int_0^{z_s} dz w_1(z, z_s) \frac{(1+z)}{E(z) d_L(z)^2} \int_0^\infty dL L \phi(L, z) \Phi(L, z) \quad (3)$$

$$E(z) \equiv [\Omega_m(1+z)^3 + (1 - \Omega_m - \Omega_\Lambda)(1+z)^2 + \Omega_\Lambda]^{1/2} \quad , \quad \chi(z) = \frac{1}{H_o} \int_0^z \frac{dz'}{E(z')} \quad (4)$$

where  $\eta(z)$  is the number density (number per proper volume) of observed galaxies,  $d_L(z)$  is the luminosity distance,  $\phi(L, z)$  is the selection function of the survey and  $\Phi(L, z)$  is the luminosity function in comoving volume. The comoving radial distance is  $\chi(z)$ . The selection function,  $\phi(L, z)$ , will depend on details of the particular survey. In the numerical calculations shown later a simple flux limited survey will be assumed where  $\phi(L, z)$  zero for  $L < L_c(z)$  and one for larger  $L$ . In terms of the flux limit  $L_c(z) = 4\pi d_L(z)^2 f_c$ . The luminosity function of detectable galaxies,  $\phi(L, z) \Phi(L, z)$ , can be found empirically and independently of the SNe.

A SN is an unresolved near–point source so the only observable effects of gravitational lensing are image magnification and the multiplication of images. If DM is microscopic as is assumed here the probability of a SN at  $z \simeq 1$  having multiple, distinguishable images is very small ( $< 10^{-4}$ ). Except for rare cases, SNe will be only weakly magnified and demagnified by matter very close to the line-of-sight and no multiple images will occur. To second order the magnification,  $\mu = 1 + 2\kappa + 3\kappa^2 + \gamma^2$ . The convergence,  $\kappa$ , is defined by its relation to the magnification matrix:  $\text{tr} A = 2(1 - \kappa)$  and the shear is  $\gamma^2 = |A - (1 - \kappa)I|$ . So in the weak lensing limit,  $\kappa, \gamma \ll 1$ , the magnification is independent of the shear. The convergence, and thus  $\mu$  in this case, depends only on the local mass density (Ricci focusing only) and can be calculated perturbatively (Kaiser 1992; Blandford et al. 1991)

$$\mu - 1 = \delta\mu \simeq \int_0^{z_s} dz W_l(z, z_s) \delta(z) \quad , \quad W_l(z, z_s) \simeq \frac{3\Omega_m H_o (1+z)}{E(z)} \frac{g[\chi(z)] g[\chi(z_s) - \chi(z)]}{g[\chi(z_s)]} \quad (5)$$

where the density contrast along the line-of-sight is  $\delta(z) = (\rho - \bar{\rho})/\bar{\rho}$ . The comoving angular size distance is  $g(\chi) = \{R_{curv} \sin(\chi/R_{curv}), \chi, R_{curv} \sinh(\chi/R_{curv})\}$  in the closed, flat and open cases. The curvature

scale is  $R_{curv}^{-1} = H_o \sqrt{1 - \Omega_m - \Omega_\Lambda}$ . This can be easily modified in everything that follows to account for strong lensing as well as weak. In this notation the luminosity distance is  $d_L(z) = (1+z)g[\chi(z)]$ .

## 2.1. Correlations

Consider the cross-correlation of  $\mathcal{F}$  with the brightness of the SN,  $b$ . At a given redshift the magnification is defined with respect to the mean brightness at that redshift. Ideally the average brightness of the standard candle,  $\bar{b}(z)$ , would be calculated from the SNe themselves. This would make the measurement of lensing independent of cosmology and any redshift evolution of the SNe. However this may not prove feasible in the short term if there are not enough SNe within a small redshift range to accurately determine the average. In this case the cosmology can be fixed so that the redshift dependence of the mean brightness is predicted. Determining the cosmological parameters can be effectively done with lower redshift SNe which are largely unaffected by lensing and with other observations. The average  $\bar{\mathcal{F}}(z)$  can be measured without regard to the presence of background SNe.

I will consider the correlation function

$$\mathcal{S}_{\mathcal{F}\mu}^2 \equiv \frac{1}{N_{sn}} \sum_j \frac{\Delta \mathcal{F}_j \Delta b_j}{\bar{\mathcal{F}}_j \bar{b}_j} \quad (6)$$

where  $\Delta b_i = b_i - \bar{b}(z_i)$ . The sum is over the sample of SNe. If the SNe are used to estimate the average  $\bar{b}(z_i)$  one must take into account the correlations in the finite sample. The averages of these statistics can be expressed in terms of the magnification of the SNe in a redshift range

$$\langle \mathcal{S}_{\mathcal{F}\mu}^2 \rangle = \langle \delta \mathcal{F} \delta \mu \rangle. \quad (7)$$

where  $\delta \mathcal{F} = (\mathcal{F} - \bar{\mathcal{F}}) / \bar{\mathcal{F}}$ .

To interpret and predict measurements of this statistic, its mean value must be related to the distribution of DM and galaxies. For these purposes I define a position-dependent luminosity function by writing the probability of a galaxy being within a comoving volume  $\delta V$  and in a range of luminosity  $\delta L$  as

$$\delta V \delta L \Phi(\vec{x}, L, z) = \delta V \delta L \Phi(L, z) [1 + \delta \Phi(\vec{x}, L; \delta_{\vec{y}})]. \quad (8)$$

The probability of a galaxy being at  $\vec{x}$  is presumably dependent on the density field,  $\delta_{\vec{y}}$ , at the point  $\vec{x}$  and in surrounding regions. This luminosity function is a *function* of position and luminosity, but a *functional* of the density field. This functional property expresses the probability that a galaxy's existence and properties depend on more than the smoothed density at its position. Nonlocal properties of the surrounding density field are probably important.

In relating these statistics to correlations of galaxies and mass density I will employ an extended Limber's approximation which requires that all such correlations are limited to scales much smaller than those over which quantities like redshift, the lensing window and the angular size distance change appreciably. With this approximation and the luminosity function above, the correlations between magnification and  $\mathcal{F}$  can be written

$$\begin{aligned} \langle \mathcal{S}_{\mathcal{F}\mu}^2 \rangle \bar{\mathcal{F}} &= \frac{1}{N_{sn}} \sum_{z_s} \frac{1}{2} \int_0^{z_s} dz w_1(z, z_s) \frac{(1+z)^3 W_l(z)}{d_L(z)^2} \int_0^\infty dL L \phi(L, z) \Phi(L, z) \int_0^\infty dy y w_2(y) \\ &\quad \times \int_{-\infty}^\infty dr \xi_{\Phi\delta}(\sqrt{y^2 + r^2}, L, z). \end{aligned} \quad (9)$$

where the last radial integral is over proper distance not comoving distance. The luminosity function – mass correlation function is defined by

$$\xi_{\Phi\delta}(|\vec{x}_1 - \vec{x}_2|, L, z) \equiv \langle \delta \Phi(\vec{x}_1, L; \delta_{\vec{y}}) \delta(\vec{x}_2) \rangle \quad (10)$$

where all quantities are evaluated at the epoch corresponding to the redshift  $z$ .

### 3. Modeling the Signal

For estimates of the lensing signal, structure in the DM distribution will be modeled as consisting of two components. First each galaxy has a DM halo surrounding it whose properties are correlated with observable properties of the galaxy. In addition, the galactic halos are clustered into clusters which contain additional mass. The lensing contributions from each of these components are considered separately in the next two subsections.

#### 3.1. Galaxy Halos

Let us make the simplifying assumption that each galaxy sits at the center of a massive halo so that  $\delta\Phi(\vec{x}, L) = -1$  everywhere but in these locations. In addition, it will be assumed that all the positions and properties of the halos are uncorrelated with each other, but directly related to the observable properties of the tenant galaxy. These assumptions are probably incorrect in detail, but they will serve well as a statistical model whose validity can be tested by the observations. The additional mass contained in groups and clusters of galaxies will be handled separately.

In this galaxy halo model the correlation function is given by

$$\xi_{\Phi\delta}(r, L, z) = \delta_h(r, L, z) = \frac{\rho_h(r, L, z)}{\bar{\rho}_o(1+z)^3} - 1, \quad (11)$$

$$\int_{-\infty}^{\infty} dr \xi_{\Phi\delta}(\sqrt{y^2 + r^2}, L, z) = \xi_{g\Sigma}(y, L, z) = \frac{\langle \Sigma_h(y, L, z) \rangle_{\Theta}}{\bar{\rho}_o(1+z)^3} \quad (12)$$

where  $\rho_h(r, L, z)$  is the density of the halo which surrounds a galaxy of luminosity  $L$  at redshift  $z$  and  $\Sigma_h(y, L, z)$  is its surface density. The average is over the orientation and substructure of the halo.

For the purposes of estimating the signal the surface density of a galactic halo will be modeled by

$$\Sigma(y) = \frac{V_c^2}{2G} \frac{1}{y(1+y/r_c)^\gamma} \quad ; \quad V_c = V_* \left( \frac{L}{L_*} \right)^\beta, \quad r_c = r_* \left( \frac{L}{L_*} \right)^\alpha. \quad (13)$$

This profile matches a singular isothermal sphere at small  $y$  and then drops away more rapidly beyond  $r_c$  with an adjustable slope. The central velocity dispersion is related to the luminosity by the Tully-Fisher relation,  $\beta \simeq 1/4$ . The scale size,  $r_c$ , is related to the luminosity by a less certain relation. In what follows  $\alpha = 1/2$  which in the case of  $\beta = 1/4$  gives a constant mass to light ratio for the isothermal part of the halos. In addition this makes  $r_c$  proportional to the radius of the visible galaxy in an idealized case where the surface brightness is a constant. The luminosity function is taken to be a Schechter function  $\Phi(xL_*) = \Phi_* x^{-1.07} e^{-x}$  with  $L_* = 10^{10} h^{-2} L_\odot$  and independent of redshift. The weighting function will be

$$w_1(z, z_s) = W_l(z, z_s) d_L(z)^2 \quad , \quad w_2(y) = \begin{cases} \frac{1}{\pi(R^2 - R_{min}^2)} & R_{min} < y < R \\ 0 & y > R, y < R_{min} \end{cases} \quad (14)$$

This is not necessarily the optimal weighting, but it does seem to give high signal to noise without prejudicing the result by assuming a specific halo profile. With this weighting function  $\mathcal{S}_{\mathcal{F}\mu}^2(R)$  is directly related to the average surface density in the annulus  $R_{min} < y < R$  surrounding a galaxy.

In the above the weak lensing approximation has been used. More generally  $\mathcal{S}_{\mathcal{F}\mu}^2(R)$  is related to the average magnification within the annulus. However the probability of forming an image is

not uniformly distributed on the image plane due to magnification bias. The result of this is that  $\mathcal{S}_{\mathcal{F}\mu}^2(R) \propto \langle \mu \rangle_{sn} - 1 = \langle \mu^{-1} \rangle_x^{-1} - 1$  where  $\langle \dots \rangle_x$  is the average over the annulus  $R_{min} < y < R$ . Weak lensing will be assumed throughout this paper so this distinction in the interpretation of  $\mathcal{S}_{\mathcal{F}\mu}^2(R)$  will not be important.

### 3.2. Extragalactic Clustering

It is well established that in the central regions of galaxy clusters most of the mass is not associated with individual galaxies but resides in intergalactic space. This is confirmed by observations of gravitational lensing using galaxy shear (Natarajan et al. 1998), the Sunyaev-Zel’dovich effect and X-ray emission. This extra cluster mass can have significant lensing effects and conversely any information that can be gained through lensing on the structure of clusters would contribute to our understanding of cluster formation and evolution.

To model the effects of extragalactic mass - mass outside of any galactic halo - I treat the galaxy halos as being embedded in larger halos with a universal profile but of varying size and mass. Only the component of extragalactic mass that resides in virialized halos will be considered because any other component will not contribute appreciably to the lensing considered here. Because  $\delta\mu \propto \Sigma$  to first order the contribution of the extragalactic mass to lensing can then be calculated separately and simply added to the contribution from galactic halos. This will not be true for strongly lensed SNe, but these are comparatively rare and will not be considered here. I will call the extragalactic contribution the cluster contribution although it will include extragalactic halos with masses well below what is normally called a galaxy cluster. The division between galactic and cluster mass is somewhat arbitrary in any particular case, but it does have a meaning in a statistical sense. By comparing cluster galaxies with the ‘average’ galaxy the extra mass can be attributed to the cluster or group. This separation is more direct and less model dependent than it is for shear measurements (see Natarajan, Kneib, & Smail 1999; Natarajan et al. 1998) owing to the magnification being directly proportional to the surface density.

The relative mass density of an extragalactic halo is written  $\delta_c(\vec{x}, M)$  and its projection onto two dimensions is  $\delta\Sigma_c(\vec{y}, M)$ . If the density of galaxies is assumed to be proportional to the overdensity the correlation on the sky between galaxies and surface density in halos with masses between  $M$  and  $M + dM$  is given by

$$\xi_{g\Sigma}^{cl}(y, M) = f_\Sigma(M) f_g(M) \int \frac{d\theta_y}{2\pi} \int d^2x \delta\Sigma_c(\vec{x}, M) \delta\Sigma_c(\vec{x} - \vec{y}, M) / \int d^3x \delta_c(\vec{x}, M) \quad (15)$$

$$= \frac{f_\Sigma(M) f_g(M)}{\delta\Sigma_c(0, M)} \int \frac{dk k}{2\pi} J_o(ky) |\delta\Sigma_c(k, M)|^2 \quad (16)$$

where  $f_g(M)$  is the fraction of galaxies in halos within this mass range and  $f_\Sigma(M)$  is the fraction of the cluster surface density that is not in any galaxy halo. The first integral in (15) is an average over the direction of  $\vec{y}$  or equivalently the orientation of the halo. It is often more convenient to calculate the correlation function from the Fourier transform of the halo profile,  $\delta\Sigma_c(k, M)$ . If the weight function  $w_2(y)$  is given by (14) with  $R_{min} = 0$ , a top hat, the relevant quantity is the average correlation function within a circle of radius  $R$ ,

$$\overline{\xi_{g\Sigma}^{cl}}(M, R) = \frac{f_\Sigma(M) f_g(M)}{\pi R \delta\Sigma_c(0, M)} \int dk J_1(kR) |\delta\Sigma_c(k, M)|^2. \quad (17)$$

The  $J$ ’s are Bessel functions.

Computationally the problem can be simplified when the halo profile obeys the scaling law

$$\delta\Sigma_c(k, M) = \delta_o(M) r_{cl}(M)^3 \delta\Sigma_c(r_{cl}(M)k) \quad ; \quad \xi_{g\Sigma}^{cl}(y, M) = f_\Sigma(M) f_g(M) \delta_o(M) r_{cl}(M) \hat{\xi}_{g\Sigma}^{cl}\left(\frac{y}{r_{cl}(M)}\right) \quad (18)$$

where  $r_{cl}(M)$  is the scale length of the halo and  $\delta_o(M)$  is a density scale. Many popular profiles are of this generic type. The scaling implies a contribution to  $\mathcal{S}_{\mathcal{F}\mu}^2$  from extragalactic halos of

$$\begin{aligned} \langle \mathcal{S}_{\mathcal{F}\mu}^2 \rangle = & \frac{1}{\overline{\mathcal{F}N_{sn}}} \sum_{z_s} \frac{1}{4\pi} \int_0^{z_s} dz w_1(z, z_s) \frac{(1+z)^3 W_l(z)}{d_L(z)^2} \int_0^\infty dL L \phi(L, z) \Phi^{cl}(L, z) \\ & \times \int_{M_{min}}^\infty dM f_\Sigma(M, z) f_g(M, z) \delta_o(M, z) r_{cl}(M, z) \overline{\hat{\xi}_{g\Sigma}^{cl}} \left( \frac{R}{r_{cl}(M, z)} \right). \end{aligned} \quad (19)$$

This scaling allows one to calculate  $\overline{\hat{\xi}_{g\Sigma}^{cl}}(x)$  once and then integrate over halo mass and redshift. The mass  $M_{min}$  is the mass of the smallest halo that contains multiple galaxies. The luminosity function is given a superscript because there is a known segregation of galaxy types between clusters and the field. However in the calculations to follow I take the cluster galaxies to have the same luminosity function and halo distribution as the galaxies in the field.

For signal estimates I will assume the extragalactic clusters are of the Navarro, Frenk and White (NFW) form (Navarro, Frenk, & White 1997, 1996):

$$\delta_{cl}(r) = \frac{\delta_o}{(r/r_{cl})(1 + r/r_{cl})^2}. \quad (20)$$

The average galaxy-surface density correlation function,  $\overline{\hat{\xi}_{g\Sigma}^{cl}}(x)$ , in this model is plotted in figure 1. This function is effectively constant for  $x \lesssim 0.1$  and zero for  $x \gtrsim 10$ .

To calculate (19) some assumptions concerning the population of halos and their galaxy content must be made. I will consider flat CDM models with scale free ( $n = 1$ ) initial perturbations. The parameters  $\delta_o(M, z)$  and  $r_c(M, z)$  are related by  $r_c = r_{200}(M)/c$  and  $\delta_o = \frac{200}{3\Omega_m(z)} c^3 / [\ln(1+c) - c/(1+c)]$  where  $r_{200}(M)$  is the radius within which the mean density is 200 times the background. To simplify the procedure of calculating these quantities the simple formula  $c \simeq c_*(M/M_*(z))^{-0.2}$  is used. The nonlinear mass scale is defined by the condition  $\Delta_o(M_*, z) = \delta_c(z)$  where the critical density is  $\delta_c = 1.6865 \Omega_m(z)^{0.0055}$  for flat models. These scalings reasonably reproduce the results of Navarro et al. (1996). The normalizations for the  $\Lambda$ CDM model considered here ( $\Omega_m = 0.3$ ,  $\Omega_\Lambda = 0.7$ ) are  $\sigma_8 = 1.14$  and  $c_* = 7.9$ . For standard CDM ( $\Omega_m = 1$ ),  $\sigma_8 = 0.6$  and  $c_* = 10$ . The fluctuations on  $8h^{-1}$  Mpc scales,  $\sigma_8$ , is consistent with observed galaxy abundances in both models (Viana & Liddle 1996).

In populating the clusters with galaxies it is assumed that the fraction of galaxies in clusters within a given mass range is equal to the fraction of total mass which is contained in those clusters. The mass fraction can be calculated using the Press-Schechter prediction for the mass function of halos. This results in

$$f_g(M, z) = -\sqrt{\frac{2}{\pi}} \frac{\delta_c}{D(z)\Delta_o^2(M)} \frac{d\Delta_o}{dM}(M) \exp\left(\frac{-\delta_c^2}{2D(z)^2\Delta_o^2(M)}\right) \quad (21)$$

The galaxy halos are statistically the same in and out of clusters. The fraction of the mass in the cluster but not in a galactic halo,  $f_\Sigma(M, z)$ , will not depend on  $M$  in this case. The assumption that the galaxy content of a cluster is proportional to mass results in  $f_\Sigma(z) = 1 - \rho_g(z)/\bar{\rho}(z)$  where  $\rho_g(z)$  is the total mass content of galaxies and their halos. With the static halo model considered here  $f_\Sigma$  is independent of redshift. Typically  $f_\Sigma \sim 0.4$ . This number would increase if cluster galaxies are tidally truncated as they undoubtedly are in reality.

Figure 2 shows the expected size of  $\mathcal{S}_{\mathcal{F}\mu}^2(R)$  for SNe at  $z = 1$  where  $R$  is the radius of the weighting function in (14). On top are curves representing the contribution of galaxy halos. In each case an artificial inner cutoff,  $R_{min}$ , is made so that SNe whose line-of-sight comes within this distance of a galaxy are excluded in order to avoid problems with obscuration. This is an adjustable parameter that is applied

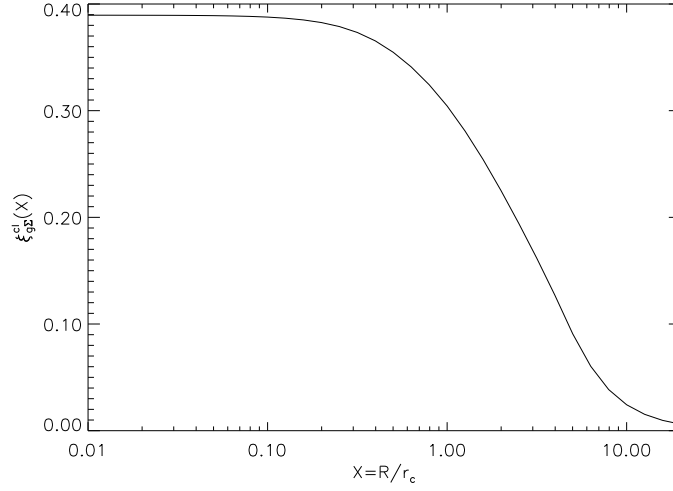


Fig. 1.— The galaxy-surface density correlation function averaged over a disk,  $\hat{\xi}_{g\Sigma}^{cl}(x)$ . The extragalactic halo is taken to be of the NFW form (equation 20).

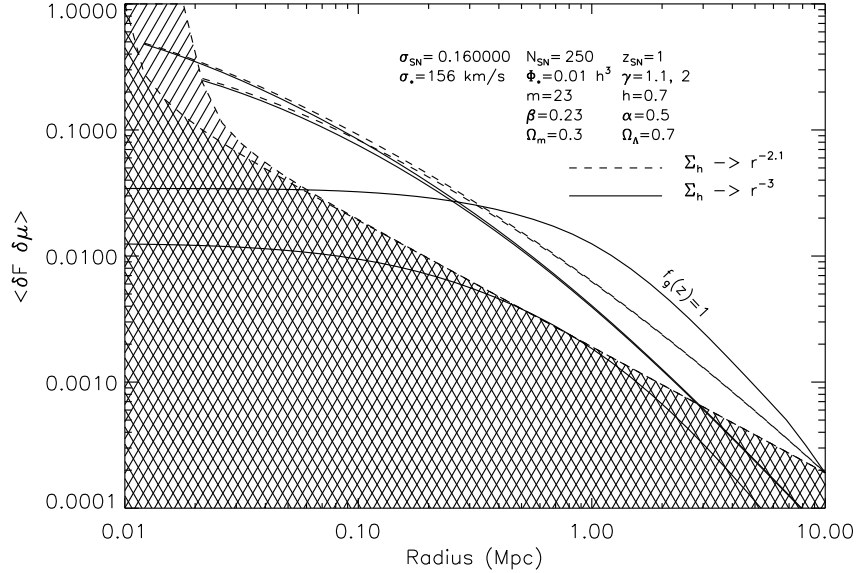


Fig. 2.— The correlation of light and magnification  $\mathcal{S}_{\mathcal{F}\mu}^2(R)$  for SNe at  $z = 1$ . The contributions from galaxy halos and extragalactic halos are plotted separately. The total  $\mathcal{S}_{\mathcal{F}\mu}^2$  is the sum of the two components. The galactic halo curves are the steeper ones starting in the upper left corner. Two different models which differ in the logarithmic slope of the surface density at large galactic radii are shown. For each model two inner cutoffs are considered –  $R_{min} = 10, 20$  kpc. All SNe within  $R_{min}$  of any galaxy are excluded. The two curves that flatten out on the left are the contributions from clusters in the CDM model. The one marked  $f_g(z) = 1$  represents the case where only SNe behind  $M > 10^{14} M_\odot$  clusters are selected. The crisscrossed region represents the uncorrelated noise contributed by uncertainties in SN peak luminosities ( $\sigma_{sn} = 0.16$  mag) and shot noise in the galaxy counts for the case of 250 SNe (see section 4). The signal to noise ratio at  $R = 200$  kpc is  $\simeq 4\sqrt{N_{sn}/250}$ . The limiting magnitude of foreground galaxies is  $m = 23$ . Additional parameters are printed on the plot.



when analyzing the data.  $\mathcal{S}_{\mathcal{F}\mu}^2(R)$  is then proportional to the average surface density between  $R_{min}$  and  $R$ . Figure 2 shows that  $\mathcal{S}_{\mathcal{F}\mu}^2(R)$  is relatively independent of  $R_{min}$  when  $R \gtrsim R_{min}$ . The inner part of these curves, beyond the  $R_{min}$ , depend only on the isothermal part of the halo model and thus only on the Tully-Fisher relation. This could in fact be a way of determining if a Tully-Fisher-Faber-Jackson type relation applies to halos. Two different halo models are shown with  $\gamma = 2$  and 1.1 (halo model is given in (13)). These models start to diverge from each other at large  $R$  ( $r_* = 500$  kpc in these models), but differentiating between them is likely to require a large number of SNe both because of the small difference and the contribution of cluster mass which starts to become significant around the same radii. It is clear in both models that  $\mathcal{S}_{\mathcal{F}\mu}^2(R)$  deviates from isothermal as  $R$  gets larger. A measurement of the halo size scale,  $r_*$ , should be possible.

The cluster contribution is represented in figure 2 by the lower curves which flattens out at small  $R$ . The lower of these curves is the contribution expected for a random sample of SNe. In the present model this contribution is fairly small relative to the noise. This is largely because of the small number of galaxies that reside in large clusters. For these calculations the minimum mass of a cluster is taken to be  $M_{min} = 3 \times 10^{12} M_\odot$ , but it is the larger clusters which give most of the signal. All else being fixed, the extragalactic halo component will be proportional to  $f_g(M)$  - the fractional galaxy content of clusters. In this way it is a measure of bias. The noise for a sample of 250 SNe is represented in figure 2 by the crisscrossed region. With this number of SNe and the level of noise assumed here the signal is  $\sim 4.5 \times \sigma$ . a detection at the  $4.5 \sigma$  at  $R \sim 0.1$  Mpc. The noise is discussed further in section 4.

The relative size of the cluster contribution can be increased by selecting SNe – or searching for SNe – which occur behind identified clusters. The upper cluster curve in figure 2 marked  $f_\Sigma = 1$  shows the level of signal if all the SN sight lines are within  $\simeq 10$  Mpc of the center of  $M > 10^{14} M_\odot$  clusters. Now the contribution from extragalactic material is comparable or greater than the contribution from galaxy halos at  $R \sim 1$  Mpc. In actuality halos within a cluster should be tidally truncated which will make the halo curve fall more rapidly with  $R$  and the cluster curve will be higher due to the redistributed matter. It would be interesting to study the tidal stripping process in this way. It is strongly dependent on the formation history of clusters. Of course the cluster mass threshold could be increased so that the cluster lensing contribution is comparatively larger. In this way the substructure in galaxy clusters can be measured very directly.

Figure 3 shows the same  $\mathcal{S}_{\mathcal{F}\mu}^2(R)$  plot with the background cosmology changed to  $\Omega_m = 1$ . The galaxy halos are the same as in figure 2. This galaxy halo signal is almost independent of cosmology. Perhaps unexpectedly  $\Lambda$  does not have a large effect even when the galaxy halo model is held fixed. This is a result of using correlations between light and magnification rather than a statistic based purely on the magnification probability distribution such as the optical depth. The magnification probability is a stronger function of the angular size distance and the density of halos while  $\mathcal{S}_{\mathcal{F}\mu}^2$  is normalized to fit the observed density of galaxies. The cluster component is a little bit bigger in the high  $\Omega_m$  models when the power spectrum is normalized to observed cluster abundances.

The modeling of extragalactic halos done here is somewhat crude. There are many ways in which it could fail to represent reality in detail. The density of galaxies within a halo is not necessarily proportional to the halo density and the total number of galaxies in a halo may not be proportional to the halo mass. It is already known that galaxies of different morphologies, colors and luminosities are biased with respect to each other. This would seem to indicate that these assumptions are not entirely correct. In addition, large clusters tend to have a central elliptical galaxy which has not been included here. This would increase the statistical weight of the cluster contribution. More sophisticated modeling is certainly possible when the data warrants it.

#### 4. Noise in $\langle \mathcal{S}_{\mathcal{F}\mu}^2 \rangle$

There are several different sources of noise that will affect the precision and accuracy of any  $\langle \mathcal{S}_{\mathcal{F}\mu}^2(R) \rangle$  measurement. First there is noise coming from the dispersion in SN luminosities and the random fluctuations in foreground light. This noise is uncorrelated with the lensing signal. The lensing structures themselves will also contribute to the noise through sample variance. The density within radius  $R$  is concentrated toward the center of the halo. The more concentrated it is the less good an estimate of the average from a finite sample is likely to be. This problem is compounded if the DM halos are not smooth but clumped into substructures. In addition errors in the redshifts of foreground galaxies will add noise. There are also observational errors and biases arising from the light curve correction to the SN peak luminosity, the host galaxy subtraction and the detection efficiency of the SN search. For lack of detailed information on future observations I will not attempt to address the last categories of noise, but I will estimate the importance of the other sources of error.

The variance in the correlation can be written

$$\langle [\mathcal{S}_{\mathcal{F}m}^2]^2 \rangle - \langle \mathcal{S}_{\mathcal{F}m}^2 \rangle^2 = \frac{1}{N_{sn} \bar{\mathcal{F}}^2} \left[ \sigma_{\mathcal{F}}^2 \sigma_b^2 + \sigma_{\mathcal{F}}^2 \left( \frac{\Delta \bar{b}}{\bar{b}} \right)^2 + \mathcal{P}_{\mathcal{F}\mu}^4 \right] \quad (22)$$

where  $\Delta \bar{b}(\Omega_m, \Omega_\Lambda)$  is the difference between the true average brightness and the one derived using the parameters;  $\Omega_m, \Omega_\Lambda$ , etc. The variance in SN brightnesses caused by intrinsic differences and observational errors is  $\sigma_b^2$ . It is assumed that the error in  $\bar{\mathcal{F}}$  is small enough that it is unimportant. The last term represents the sample variance produced by the lensing itself. All of these quantities will be redshift dependent so in a real sample they will be different for each SN.

Errors in  $\bar{b}(\Omega_m, \Omega_\Lambda)$  should always be a subdominant. This is because the cosmology will be constrained by all of the SNe observed, including those at lower redshift, so it is expected that  $\Delta \bar{b}^2 \ll \sigma_b^2$ . Of course there is always the possibility that one has chosen the wrong parameters to describe the real universe. With enough SNe one could directly calculate  $\bar{b}(\Omega_m, \Omega_\Lambda)$  within redshift bins. This would make the result independent of cosmology at the expense of increasing the  $\bar{b}(\Omega_m, \Omega_\Lambda)$  term.

The variance of  $\mathcal{F}$  is best estimated directly from data. However, to assess the noise levels expected in a hypothetical experiment it is useful to make a semi-empirical model for the variance  $\sigma_{\mathcal{F}}^2$ . If it is assumed that the internal properties of different galaxies are uncorrelated the variance is

$$\begin{aligned} \sigma_{\mathcal{F}}^2 &= \langle \mathcal{F}^2 \rangle - \bar{\mathcal{F}}^2 \\ &= \frac{2\pi}{H_o} \int_0^{z_s} dz \frac{w_1(z, z_s)^2 (1+z)^2}{[4\pi d_L(z)^2]^2 E(z)} \left\{ \int_0^\infty dL L^2 \phi(L, z) \Phi(L, z) \int_0^\infty dy y w_2(y)^2 \right. \end{aligned} \quad (23)$$

$$\left. + \frac{(1+z)^2}{2\pi} \int_0^\infty dL L \phi(L, z) \Phi(L, z) \int_0^\infty dL' L' \phi(L', z) \Phi(L', z) \int d^2 y_1 \int d^2 y_2 w_2(y_1) w_2(y_2) \right. \\ \left. \times \int_{-\infty}^\infty dr \xi_{gg} \left( \sqrt{\Delta y^2 + r^2}, z \right) \right\} \quad (24)$$

The first term (23) is from shot noise in galaxy number counts. This expression can be derived by considering the variance in the galaxy number count within a region of space small enough to contain at most one galaxy. The probability of a galaxy being in this volume is given by equation (8). Then a Poisson distribution implies

$$\langle \Phi(L) \Phi(L') \delta \Phi(\vec{x}, L) \delta \Phi(\vec{x}', L') \rangle = \Phi(L) \delta(L - L') \delta^3(\vec{x} - \vec{x}') / (1+z)^3 \quad (25)$$

where the positions  $\vec{x}$  are measured in proper coordinates. Term (23) follows from this and is plotted in figure 4 for the low  $\Omega_\Lambda$  flat model.

The second term in  $\sigma_{\mathcal{F}}^2$ , (24), is from the clustering of galaxies. It is known from observations that the correlation function of galaxies is well approximated by  $\xi_{gg}(x) = (x/r_o)^{-\gamma}$  ( $\gamma = 1.77 \pm 0.004$  and

$r_o = 5.4 \pm 1 h^{-1}$  Mpc) and independent of redshift if  $x$  is the comoving distance. With this level of clustering  $\sigma_{\mathcal{F}}^2$  is dominated by shot noise for relevant range of  $R$  so clustering contribution will be ignored.

In addition to shot noise the estimate of  $\mathcal{F}$  is limited by errors in the estimated redshifts of the foreground galaxies. These redshifts need to be estimated either photometrically or spectroscopically. This can cause errors in two ways. If one is using the weighting function (14) errors in redshift can cause  $w_1(z_i, z_s)$  to be misestimated and it can cause a galaxy that is outside the volume allowed by  $w_2(y)$  to be misidentified as inside that volume and vice versa. If necessary the latter problem can be avoided entirely by using an angular cutoff in  $w_2(y)$  instead of a proper distance cutoff as in (14). This is done at the expense of being able to interpret  $\langle \mathcal{S}_{\mathcal{F}\mu}^2(R) \rangle$  as a measure of the average surface density within distance  $R$  of a galaxy. An estimate of the uncertainty in  $\mathcal{F}$  caused by errors in  $w_1(z, z_s)$  can be found by replacing  $w_1(z, z_s)$  in (23) with  $\frac{\delta z}{(1+z)}(1+z)\frac{dw_1}{dz}(z, z_s)$  where  $\delta z/(1+z)$  is considered constant. This is also plotted in figure 4. In the case considered here  $\sigma_{redshift} \simeq 10\delta z/(1+z)\sigma_{shot\ noise}$ . At this time photometric redshifts have an accuracy of  $\delta z \sim 0.1 - 0.2$  for the relevant redshift range (Bolzonella, Miralles, & Pello' 2000). If photometric redshifts are used this noise is comparable to the shot noise contribution. With spectroscopic redshifts this noise would be unimportant. In figures 2 and 3 only the shot noise times the SN luminosity noise is shown.

The size of the sample variance depends on the structure of the halos. If the halos are very centrally concentrated, asymmetric and/or clumpy the average  $\mathcal{S}_{\mathcal{F}\mu}^2$  will strongly depend on a small number of SNe which happen to be observed through high density region. In this case  $\mathcal{S}_{\mathcal{F}\mu}^2$  may converge to its mean value very slowly and a prohibitively large number of SNe may be required to estimate it. Ignoring correlations between halos the sample variance can be written

$$\mathcal{P}_{\mathcal{F}\mu}^n = \frac{H_o^{n-3}}{\mathcal{F}_{\mathcal{F}\mu}^2} \int_0^{z_s} dz w_1(z, z_s)^2 \frac{(1+z)^n E(z)^{n-3} W_l(z, z_s)^{n-2}}{[4\pi d_L(z)^2]^2 \bar{\rho}(z)^{n-2}} \quad (26)$$

$$\times \int_0^\infty dL L^2 \phi(L, z) \Phi(L, z) \int d^2 y w_2(y)^2 B^{n-2}(L, z, z_s, y)$$

with  $n = 4$  (the  $n \neq 4$  will be useful later).

In the weak lensing limit  $B^n(L, z, z_s, y) = \langle \Sigma(L, y)^n \rangle$ . If the halo structure is perfectly correlated with the galaxy luminosity  $B^n(L, z, z_s, y) = \bar{\Sigma}(L, y)^n$ . There is undoubtedly some scatter in the luminosity–surface density relation which will increase  $\mathcal{P}_{\mathcal{F}\mu}^4$ . The scatter is not known, but if we take the scatter in the Tully–Fisher relation as a guide  $\mathcal{P}_{\mathcal{F}\mu}^4$  will be about 10% larger than the perfect correlation value. This should be added to the lower solid curve in figure 4. The sample variance would then be smaller than the first term in (22). However the scatter could well be larger than it is for the Tully–Fisher relation in which case one might hope to measure it with higher order statistics. This is discussed in section 5.1.

Another possibility is that there is a significant amount of substructure in the dark matter halos. In this case I will resort to an approximation for  $B^n(z, z_s, y)$  to simplify calculations. In order to preserve the average angular size distance the average magnification at a distance  $y$  must be the same with or without substructure. A model for substructure lensing should respect this constraint and take into account the strong lensing that may be important if subclumps have singular cores. I consider the case where all the mass in the halo is contained in randomly placed clumps each with average surface density  $\bar{\Sigma}_{sub}$ . The probability of a clump being in the line-of-sight is then  $p = \bar{\Sigma}(y)/\bar{\Sigma}_{sub}$ . Outside the clumps the magnification is zero (it depends on shear only at second order). When the halo density is large the possibility of two clumps eclipsing the line-of-sight must be taken into account. In the weak lensing limit  $B^n(z, z_s, y) \simeq p(1 + 2p) \langle \bar{\Sigma}_{sub}^n \rangle$  where only the terms of highest order in  $\bar{\Sigma}_{sub}$  have been retained. To take strong lensing into account I renormalize this by  $\langle \delta\mu^n \rangle / \langle \delta\mu \rangle^n$ . The result is

$$B^n(L, z, z_s, y) = \begin{cases} \bar{\Sigma}(y)^n & , \text{ no substructure} \\ \frac{\langle \delta\mu(z)^n \rangle}{\langle \delta\mu(z) \rangle^n} \bar{\Sigma}_{sub}^{n-1} \bar{\Sigma}(L, y) \left( 1 + 2\bar{\Sigma}_{sub}^{-1} \bar{\Sigma}(L, y) \right) & , \text{ substructure} \end{cases} \quad (27)$$

If a magnification cutoff is imposed to make  $\langle \delta\mu^n \rangle$  converge,  $\langle \delta\mu \rangle^n$  is still calculated without this cutoff so that the proper normalization is retained.

To model the magnification within a subclump I use the solution for an isothermal sphere cutoff at an outer radius,  $R_{sub}$ . The characteristic length scale for such a lens is  $x_o = 4\pi v_c^2 D_l D_{ls} / D_s$ . The magnification, including both images, is then a function of only the rescaled impact parameter  $x = y/x_o$ :

$$\delta\mu = \begin{cases} (2-x)/x & , x < 1 \\ 1/x & , 1 < x < x_m \\ 0 & , x > x_m \end{cases} \quad (28)$$

The second moment is logarithmically divergent so a maximum magnification cutoff must be imposed to calculate (26). This cutoff can be set high enough that the probability of there being a SN in the observed sample with a magnification this high is very small. The divergence of the moments is of course not real. In actuality the finite size of the source puts a limit on the magnification.

The size of dark subclumps is not very well constrained by observations, but they do appear in simulations. Moore et al. (1999a) find a large number of subclumps in their CDM simulations - many more than are accounted for by visible dwarf galaxies. For these simple estimates I take the velocity dispersion to be  $v_c = 15 \text{ km s}^{-1}$  and the size to be 100 pc. This is an extreme model since all the mass is in rather large subclumps, but it has the advantage of simplicity and gives a conservative estimate for the noise. The sample variance,  $\mathcal{P}_{\mathcal{F}\mu}^4(R)$ , with and without this substructure is plotted in figure 4. The cutoff is set at  $\delta\mu > 10$ . In this model there is about a  $4 \times 10^{-4}$  chance of a SN at  $z = 1$  being magnified above this limit.

With the variance expected in the corrected SN luminosities the uncorrelated noise, the first term in (22), generally dominates over the sample variance. At small  $R$  the sample variance may be comparable to the uncorrelated noise, but to some extent this is a result of the model used here. One would expect the subclumps to break up when the density is high which is not reflected in the model. Another reason to think that this is an overestimate of the sample variance is that the density profiles of real CDM clumps are probably not as steep as  $\rho \propto r^{-2}$  at small  $r$ . It has recently been claimed that  $\rho \propto r^{-1.5}$  is a better approximation (Moore et al. 1999b) and the NFW model has  $\rho \propto r^{-1}$ . In these cases  $\mathcal{P}_{\mathcal{F}\mu}^4$  would be smaller.

There is one other outstanding problem that could still cause trouble for this measurement. It has been suggested that an exceptional kind of dust could account for the observed faintness of high redshift SNe. The dust grains would need to be large enough to avoid the constraints on reddening (Aguirre 1999; Perlmutter et al. 1999) and quite uniformly distributed in the intergalactic medium (Croft et al. 2000). This is not consistent with the properties of known dust, but it does remain a possibility. The distribution of this dust would presumably be correlated with galaxies so it would show up as an anti-correlation between foreground light and SN brightness. Looking for correlations might actually be the best way of testing this hypothesis as well.

In summary it seems promising that  $\langle \mathcal{S}_{\mathcal{F}\mu}^2 \rangle$  could be measured with  $\sim 250$  at  $z \simeq 1$ . If the SNe are observed with a future satellite it is likely that the noise will be smaller than is assumed here because in this case  $\sigma_{sn}$  will be smaller at high redshift.

## 5. Higher Order Correlations

The above discussion of sample variance leads to the question of whether dark subclumps in galaxy halos might be detectable through the gravitational lensing of SNe. Such a detection would have important implications for structure formation theories. Recent high resolution N-body simulations have revealed that the CDM models have several apparent problems when compared to observations. One such problem is that galaxy halos in simulations have much more substructure or smaller clumps within them than observed

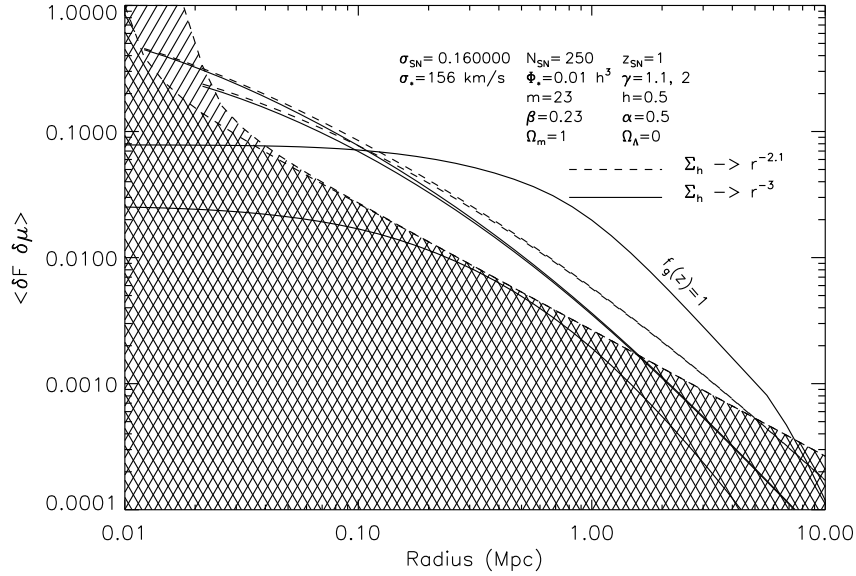


Fig. 3.— The same as in figure 2 except  $\Omega_m = 1$ ,  $h = 0.5$  and  $\sigma_8 = 0.6$ .

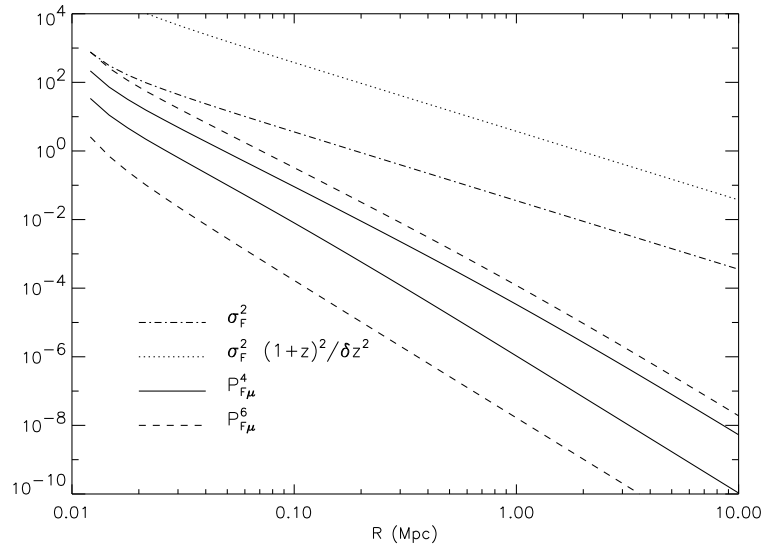


Fig. 4.— The major sources of noise for the statistics  $\mathcal{S}_{\mathcal{F}\mu}^2$  and  $\mathcal{R}_{\mathcal{F}\mu}^2$ . These are all calculated with the parameters used for figure 2. The dotted curve is the noise just from errors in redshift times  $(1+z)^2/\delta z^2$  which is regarded as a constant. The dot-dashed curve is the noise from shot noise in the galaxy counts. For each pair of  $\mathcal{P}_{\mathcal{F}\mu}^n$  curves the lower one is without substructure and the higher one has substructure. The substructure clumps, as described in the text, are truncated isothermal spheres with radius  $R_{sub} = 0.1$  kpc and velocity dispersion  $v_c = 15$  km s<sup>-1</sup>. The magnification cutoff for  $\mathcal{P}_{\mathcal{F}\mu}^4$  and  $\mathcal{P}_{\mathcal{F}\mu}^6$  is set at  $\delta\mu = 10$ . All quantities are dimensionless.

galaxies have observable dwarf satellites (Moore et al. 1999a). These subclumps form early and fall into the larger halos without being destroyed by tidal stripping and collisions. Subclumps of dwarf galaxy size seem to be over produced by about a factor of 50 in halos that should host Milky Way–like galaxies. Considering the successes of the CDM model it seems reasonable to entertain the possibility that these subclumps exist, but are dark either because they never formed stars or because their star formation was shutoff early.<sup>1</sup>

In this section I investigate the two third-order correlation functions of  $\delta\mu$  and  $\mathcal{F}$  and find that one is sensitive to this substructure. The other contains additional information on the clustering of dark matter on extragalactic scales.

### 5.1. Light-magnification-magnification Correlation

In direct analogy to  $\mathcal{S}_{\mathcal{F}\mu}^2$  I define the statistic  $\mathcal{R}_{\mathcal{F}\mu}^3$ :

$$\mathcal{R}_{\mathcal{F}\mu}^3 \equiv \frac{1}{N_{sn}} \sum_j \frac{\Delta\mathcal{F}_j \Delta b_j^2}{\bar{\mathcal{F}}_j \bar{b}_j^2} \quad , \quad \langle \mathcal{R}_{\mathcal{F}\mu}^3 \rangle = \langle \delta\mathcal{F} \delta\mu^2 \rangle \quad (29)$$

Like  $\mathcal{S}_{\mathcal{F}\mu}^2$  the average of this statistic will be zero in the absence of lensing.

Assuming weak lensing the average value of  $\mathcal{R}_{\mathcal{F}\mu}^3$  is

$$\begin{aligned} \langle \mathcal{R}_{\mathcal{F}\mu}^3 \rangle \bar{\mathcal{F}} &= \frac{H_o}{2N_{sn}} \sum_{z_s} \int_0^{z_s} dz \, w_1(z, z_s) \frac{(1+z)^4 E(z) W_l(z)^2}{d_L(z)^2} \int_0^\infty dL \, L \phi(L, z) \Phi(L, z) \int_0^\infty dy \, y w_2(y) \\ &\quad \times \int_{-\infty}^\infty \int_{-\infty}^\infty dr_1 dr_2 \, \zeta_{\Phi\delta\delta} \left( y, \sqrt{y^2 + r_1^2}, \sqrt{y^2 + r_2^2}, L, z \right). \end{aligned} \quad (30)$$

$$\zeta_{\Phi\delta\delta}(x_1, x_2, x_3, L, z) = \langle \delta\Phi(\vec{x}_1, L; \delta_{\vec{y}}) \delta(\vec{x}_2) \delta(\vec{x}_3) \rangle$$

$\mathcal{R}_{\mathcal{F}\mu}^3$  is related to how fluctuations in mass density, instead of just the mass density, are correlated with light. Taking each galaxy halo to be independent and thin results in the third order analog of equation (12)

$$\int_{-\infty}^\infty \int_{-\infty}^\infty dr_1 dr_2 \, \zeta_{\Phi\delta\delta} \left( y, \sqrt{y^2 + r_1^2}, \sqrt{y^2 + r_2^2}, L, z \right) = \frac{\langle \Sigma_h(y, L, z)^2 \rangle_\Theta}{\bar{\rho}_o^2 (1+z)^6}. \quad (31)$$

The second moment of the surface density will differ from simply the square of the average halo profile because of scatter in the  $L$ – $\Sigma$  relation, asymmetries and substructure. Asymmetries may increase the moment by a small factor. Scatter  $L$ – $\Sigma$  relation could potentially be larger – perhaps a factor of a few. Substructure could potentially have a largest effect. I use the substructure model discussed in section 4 to estimate how sensitive  $\mathcal{R}_{\mathcal{F}\mu}^3$  is to substructure. The resulting calculation is plotted in figure 5.

The variance in  $\mathcal{R}_{\mathcal{F}\mu}^3$  can be written

$$\langle [\mathcal{R}_{\mathcal{F}\mu}^3]^2 \rangle - \langle \mathcal{R}_{\mathcal{F}\mu}^3 \rangle^2 = \frac{1}{N_{sn}} (\sigma_{\mathcal{F}}^2 \mu_\mu^4 + \mathcal{S}_{\mathcal{F}\mu}^2 \mathcal{Q}_{\mathcal{F}\mu}^4 + \mathcal{P}_{\mathcal{F}\mu}^3 \mu_\mu^3 + \mathcal{P}_{\mathcal{F}\mu}^4 \sigma_b^2 + \mathcal{P}_{\mathcal{F}\mu}^6) \quad (32)$$

where  $\mathcal{P}_{\mathcal{F}\mu}^n$  is defined in (26) and

$$\mathcal{Q}_{\mathcal{F}\mu}^4 = \frac{H_o^2}{4\pi\bar{\mathcal{F}}} \int_0^{z_s} dz \, w_1(z, z_s) \frac{(1+z)^5 E(z)^2}{d_L(z)} W_l(z, z_s)^3 \int_0^\infty dL \, L \phi(L, z) \Phi(L) \int d^2y \, w_2(y) B^2(L, z, z_s, y). \quad (33)$$

---

<sup>1</sup>It is interesting to note that if this is the case the present microlensing results do not put very strong constraints on the fraction of the halo in MACHOs (see Metcalf & Silk 1996).

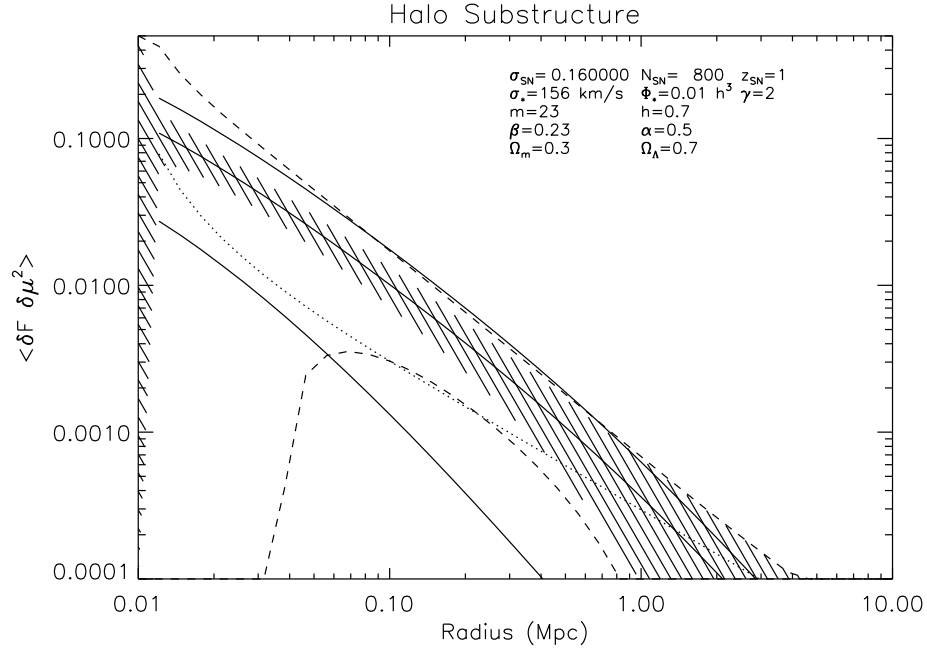


Fig. 5.— The three solid lines are the second order correlation function  $\mathcal{R}_{\mathcal{F}m}^3$ . The lowest of these is the result with no halo substructure and perfect correlation of the halo with the luminosity of its resident galaxy. The dotted curve is the noise in this case. The scatter would need to increase  $\mathcal{R}_{\mathcal{F}m}^3$  by a factor of several for it to be measurable. The other curves include substructure in the halos. The top solid curve is the result with  $\delta\mu > 10$  excluded. All the other curves are for  $\delta\mu > 4$  excluded. The inner crossed region represents the noise without sample variance. The dashed lines are the one- $\sigma$  noise with sample variances. These are all calculated for 800 SNe at  $z = 1$ .

The approximated value of  $B^2(L, z, z_s, y)$  is given in (27). The moments of the distribution of intrinsic SN luminosities are  $\mu_\mu^n$ . This distribution will be approximated as Gaussian in which case  $\mu_\mu^3 = 0$  and  $\mu_\mu^4 = 3\sigma_\mu^4$ . In reality each of these factors will be different for each SN because of differences in redshifts and observations so an average over SNe will be done.

Unlike in the case of  $\mathcal{S}_{\mathcal{F}\mu}^2$  the noise in  $\mathcal{R}_{\mathcal{F}\mu}^3$  is usually dominated by sample variance rather than SN luminosity errors and galaxy count noise. As a result both the signal and noise are strongly dependent on the structure of the subclumps. This is a result of the strongly peaked central density of the subclumps. Specifically the  $\mathcal{P}_{\mathcal{F}\mu}^6$  term in (32) tends to dominate. If the cutoff in  $\delta\mu$  is high the sample variance will swamp the signal. As can be seen in figure 5 if there is no substructure  $\langle \mathcal{R}_{\mathcal{F}\mu}^3 \rangle$  is too small to be measured with 800 SNe at  $z \simeq 1$  because of sample variance. Substructure increases the signal, but also the sample variance. A magnification cutoff can be used to reduce the sample variance without reducing the signal as significantly. The cutoff is a censoring of the data in order to improve the convergence of the remaining subsample. The high magnification events are rare so if the cutoff is at high magnification the subsample is likely to contain all the data. The subsample can be viewed as sampling the area on the surface of the halo where the magnification is below  $\delta\mu_{max}$ . By adjusting  $\delta\mu_{max}$  we can choose to have a more precise result relating to a restricted area or a less precise result relating to more of the area.

The sample variance may not be as big a problem in reality as it is in this model of substructure. Pure CDM simulations indicate that the density in the clump cores is not as steep a function of radius as in the singular isothermal sphere model (Navarro et al. 1996; Moore et al. 1999b). The density is more likely to go as  $r^{-1.5}$  or  $r^{-1}$  rather than  $r^{-2}$ . This reduces  $\langle \mathcal{R}_{\mathcal{F}\mu}^3 \rangle$ , but it reduces the sample variance more significantly. On the other side, galaxy halos are not likely to be made entirely of such large subclumps. Moore et al. (1999a) find that subclumps in their simulations have a mass distribution  $dn/dm \propto m^{-2}$  down to their resolution limit. Smaller or fewer subclumps would reduce the signal by approximately the covering fraction of the clumps.

## 5.2. Light-light-magnification correlation

Finally, for completeness, there is the light-light-magnification correlation function

$$\mathcal{I}_{\mathcal{F}\mu}^3 \equiv \frac{1}{N_{sn}} \sum_j \frac{\Delta \mathcal{F}_j^2 \Delta b_j}{\overline{\mathcal{F}_j^2} \overline{b_j}} \quad , \quad \langle \mathcal{I}_{\mathcal{F}\mu}^3 \rangle = \langle \delta \mathcal{F}^2 \delta \mu \rangle \quad (34)$$

$$\begin{aligned} \langle \mathcal{I}_{\mathcal{F}\mu}^3 \rangle \overline{\mathcal{F}^2} &= \frac{1}{N_{sn}} \sum_{z_s} \int_0^{z_s} dz w_1(z, z_s)^2 \frac{(1+z)^6 W_1(z)}{[4\pi d_L(z)^2]^2} \int_0^\infty dL L \phi(L, z) \Phi(L, z) \int_0^\infty dL' L' \phi(L', z') \Phi(L', z) \\ &\times \int_{-\infty}^\infty d^3 r \int_{-\infty}^\infty d^3 r' w_2(r_\perp) w_2(r'_\perp) \zeta_{\Phi\Phi\delta} \left( |\vec{r}|, |\vec{r}'|, |\vec{r} - \vec{r}'|, L, L', z \right) \end{aligned} \quad (35)$$

$$\zeta_{\Phi\Phi\delta}(x_1, x_2, x_3, L, L', z) = \langle \delta\Phi(\vec{x}_1, L; \delta_{\vec{y}}) \delta\Phi(\vec{x}_2, L'; \delta_{\vec{y}}) \delta(\vec{x}_3) \rangle \quad (36)$$

The integrals over the third order correlation function  $\zeta_{\Phi\Phi\delta}(x_1, x_2, x_3, L, L', z)$  can be expressed as the sum of two terms. One is a shot noise term resulting from galaxy halos taken individually. Like  $\langle \mathcal{S}_{\mathcal{F}\mu}^2 \rangle$  this term is proportional to the galaxy-surface-density correlation function. Then there is a term from correlations between different galaxies which is proportional to the galaxy-galaxy-surface-density correlation function. This term falls off less rapidly with  $R$  so that at large radii  $\langle \mathcal{I}_{\mathcal{F}\mu}^3 \rangle$  is related to the average surface density associated with multiple galaxies.

It was shown in section 3.2 that by selecting (or searching for) SNe that are seen through galaxy clusters  $\mathcal{S}_{\mathcal{F}\mu}^2(R)$  can be used as a probe of cluster matter. The selection process would likely have a rather high cluster mass threshold. To probe smaller mass clusters and halos a more systematic approach



might be useful. The statistic  $\mathcal{I}_{\mathcal{F}\mu}^3(R)$  provides a more direct, although somewhat noisier, way of probing extragalactic halo structure. This will not be feasible until a considerable number SNe have been observed so no detailed calculations of  $\langle \mathcal{I}_{\mathcal{F}\mu}^3 \rangle$  will be attempted here.

## 6. Comparison with the lensing of galaxies and quasars

The gravitational lensing of galaxies is now an established field of observational astronomy. It is appropriate that the lensing of SNe be compared with that of galaxies to argue for their independence and complementarity. Weak lensing can be detected either through the distortion of galaxy images or variations in their number counts. The former is a measure of the shear field and the latter is a measure of the magnification. Galaxy–galaxy lensing, the technique most similar to the one discussed here, is where the image distortion of background galaxies is correlated with their projected distances from foreground galaxies. This results in a measurement of the average shear as a function of distance from a galaxy. Such measurements have been done or attempted by several groups (Fischer et al. 1999; Hudson et al. 1998; Brainerd et al. 1996; Griffiths et al. 1996; Tyson et al. 1984). The tangential shear averaged around any circle on the sky of radius  $\theta$  is given by the remarkably simple relation  $\bar{\gamma}_t(\theta) = \bar{\kappa}(<\theta) - \bar{\kappa}(\theta)$  where  $\kappa(\theta) = \Sigma(\theta)/\Sigma_c(z, z_s)$  is the convergence. The average convergence within the circle is  $\bar{\kappa}(<\theta)$  and the average on the circle is  $\bar{\kappa}(\theta)$ . In the weak lensing limit  $\delta\mu(\vec{\theta}) = 2\kappa(\vec{\theta})$  so for a singular isothermal sphere  $\bar{\gamma}_t(\theta) = \bar{\kappa}(\theta)$  and  $\delta\mu(\vec{\theta}) \simeq 2\bar{\gamma}_t(\theta)$ . If the mass profile falls off more rapidly than isothermal, as it must for the mass to be finite,  $\delta\mu(\vec{\theta})$  will fall off more steeply than  $\bar{\gamma}_t(\theta)$ . For this reason measuring  $\delta\mu(r)$  with SNe might be a better method for finding the size of galaxy halos. Galaxy–galaxy lensing has not been able to put any clear constraint on the size of halos. The transition between galaxy halos and intercluster material might also be more distinct with SNe.

The shear and magnification measurements could also be combined; galaxy–galaxy lensing constraining mostly the mass scale of halos and SN lensing the size scale. In this way degeneracies and systematic errors could be significantly reduced. The signal to noise per source is actually better for SNe than for galaxies. The rms ellipticity of galaxies is  $\langle \epsilon^2 \rangle^{1/2} \simeq 0.3$  so for isothermal lenses roughly 10–25 times the number of background galaxies as SNe are needed to attain the same signal to noise. This factor brings the number of require SNe into the range that is already being considered for measuring cosmological parameters.

As discussed in section 5.1 there is the possibility of measuring substructure in galactic halos with SNe. Because the image sizes of the background galaxies are generally much larger than the size of subclumps galaxy–galaxy lensing will not be able to measure any realistic level of substructure. In addition, the contributions to the shear from the halo as a whole and the subclumps are incoherent. In contrast the lensing of SNe is sensitive to substructure masses all the way down to a small fraction of a solar mass.

Another use for the lensing of galaxies is to actually map the shear field. Because each galaxy has an intrinsic ellipticity the shear can only be measured in cells which contain multiple galaxies. This limits the angular resolution on which the shear field can be mapped. The same is true for magnification bias where the number density of background galaxies is related to the magnification. The lensing of SNe is unlikely to ever be useful for this kind of study because the number density on the sky will always be significantly lower than the number density of galaxies. However, SNe may be used to remove the mass sheet degeneracy that exists in shear maps of galaxy clusters (Kolatt & Bartelmann 1998).

Quasars have been used as sources in lensing studies for years. They are similar to SNe in that they are nearly point sources, but they are not standard candles. As a result lensing is only detectable when multiple images are formed. This is a rare occurrence and tells use more about the central regions of halos than their outskirts. Monitoring the light curves of multiple images does seem to be a promising method for detecting compact objects. Subclumps the size of dwarf galaxies however will have time scales that are

to long to be detected in this way.

## 7. Discussion

It has been shown that gravitational lensing can be measured by correlating SN brightnesses with the density of foreground galaxies. The result is a measure of the correlation of mass with light, the bias, on  $\sim$  Mpc scales. The size and mass scales of galaxy halos should be measurable with a few hundred SNe at  $z \sim 1$ . The structure of galaxy clusters can also be probed by selecting SNe that are viewed through clusters. Higher order correlations can be used to probe substructure in galaxy halos. In this case the convergence of the result is strongly dependent on the form of the substructure that is present.

The prospects for making these measurements seem very good. The numbers of SNe and the noise levels discussed in this paper are attainable, even conservative. The proposed VISTA telescope is expected to be able to find hundreds of SNe at redshifts  $\gtrsim 1$ .<sup>2</sup> The proposed SNAPSAT satellite could find thousands up to  $z \simeq 1.7$ .<sup>3</sup> At high redshift the major source of uncertainty in a SN luminosity comes from subtracting the light of the host galaxy. The superior resolution of a satellite could reduce the variance in the corrected peak luminosities of high redshift SNe to that of local SNe,  $\Delta m \simeq 0.12$  mag or better. This would be a significant improvement on the  $\Delta m \simeq 0.16$  mag assumed throughout this paper. Gravitational lensing adds strongly to the motivations for these projects.

I would like to thank D. Mortlock and P. Natarajan for very helpful comments on this paper.

## REFERENCES

- Aguirre, A. 1999, ApJ, 525, 583
- Blandford, R. D., Saust, A. B., Brainerd, T. G., & Villumsen, J. V. 1991, MNRAS, 251, 600
- Bolzonella, M., Miralles, J., & Pello', R. 2000, preprint, astro-ph/0003380
- Brainerd, T. G., Blandford, R. D., & Smail, I. 1996, ApJ, 466, 623
- Croft, R. A. C., Davè, R., Hernquist, L., & Katz, N. 2000, preprint, astro-ph/0002422
- Dyer, C. C. & Roeder, R. C. 1974, ApJ, 189, 167
- Fischer, P., McKay, T., Sheldon, E., Connolly, A., Stebbins, A., Frieman, J., Jain, B., Joffre, M., et al., 1999, preprint, astro-ph/9912119
- Griffiths, R. E., Casertano, S., Im, M., & Ratnatunga, K. U. 1996, MNRAS, 282, 1159
- Hamuy, M., Phillips, M. M., Suntzeff, N. B., Schommer, R. A., Maza, J., Antezan, A. R., Wischnjewsky, M., Valladares, G., et al., 1996, AJ, 112, 2408
- Hudson, M. J., Gwyn, S. D. J., Dahle, H., & Kaiser, N. 1998, ApJ, 503, 531
- Kaiser, N. 1992, ApJ, 388, 272
- Kochanek, C. S. 1996, ApJ, 457, 228

---

<sup>2</sup>home page: <http://www-star.qmw.ac.uk/~jpe/vista/>

<sup>3</sup>home page: <http://snap.lbl.gov/proposal/>

- Kolatt, T. S. & Bartelmann, M. 1998, *MNRAS*, 296, 763
- Metcalfe, R. B. 1998, in *Evolution of Large-Scale Structure: From Recombination to Garching*, ed. A. Banday, R. Sheth, & L. da Costa, E25, astro-ph/9810440
- Metcalfe, R. B. 1999, *MNRAS*, 305, 746
- Metcalfe, R. B. & Silk, J. 1996, *ApJ*, 464, 218
- Metcalfe, R. B. & Silk, J. 1999, *ApJ*, 519, L1
- Moore, B., Ghigna, S., Governato, F., Lake, G., Quinn, T., Stadel, J., & Tozzi, P. 1999a, *ApJ*, 524, L19
- Moore, B., Quinn, T., Governato, F., Stadel, J., & Lake, G. 1999b, *MNRAS*, 310, 1147
- Natarajan, P., Kneib, J., & Smail, I. 1999, in *Gravitational Lensing: Recent Progress and Future Goals*, ed. T. G. Brainerd & C. S. Kochanek, astro-ph/9909349
- Natarajan, P., Kneib, J. P., Smail, I., & Ellis, R. S. 1998, *ApJ*, 499, 600
- Navarro, J. F., Frenk, C. S., & White, S. D. M. 1996, *ApJ*, 462, 563
- . 1997, *ApJ*, 490, 493
- Perlmutter, S., Aldering, G., Goldhaber, G., Knop, R. A., Nugent, P., Castro, P. G., Deustua, S., Fabbro, S., et al., 1999, *ApJ*, 517, 565
- Perlmutter, S., Gabi, S., Goldhaber, G., Goobar, A., Groom, D. E., Hook, I. M., Kim, A. G., Kim, M. Y., et al., 1997, *ApJ*, 483, 565
- Porciani, C. & Madau, P. 2000, *ApJ*, 532, 679
- Rauch, K. P. 1991, *ApJ*, 374, 83
- Riess, A. G., Filippenko, A. V., Challis, P., Clocchiatti, A., Diercks, A., Garnavich, P. M., Gilliland, R. L., Hogan, C. J., et al., 1998, *AJ*, 116, 1009
- Riess, A. G., Press, W. H., & Kirshner, R. P. 1996, *ApJ*, 473, 88
- Seljak, U. & Holz, D. E. 1999, *A&A*, 351, L10
- Tyson, J. A., Valdes, F., Jarvis, J. F., & Mills, A. P. 1984, *ApJ*, 281, L59
- Viana, P. T. P. & Liddle, A. R. 1996, *MNRAS*, 281, 323
- Wilkinson, M. I. & Evans, N. W. 1999, *MNRAS*, 310, 645
- Zaritsky, D. & White, S. D. M. 1994, *ApJ*, 435, 599